33rd Annual International Conference of the IEEE EMBS
Boston, Massachusetts USA, August 30 - September 3, 2011

Detection and Removal of Stimulation Artifacts in Electroencephalogram Recordings

Ulrich Hoffmann, Woosang Cho, Ander Ramos-Murguialday, and Thierry Keller

Abstract— **Stimulation artifacts are short-duration, high-amplitude spikes which can be observed in electroencephalogram (EEG) recordings whenever surface functional electrical stimulation (FES) is applied during recordings. Stimulation artifacts are of non-physiologic origin and hence have to be removed before analysis of the EEG can take place. In this paper, algorithms for the detection and removal of stimulation artifacts are presented. The algorithms require only little computational resources and can be applied online, while signals are recorded. Therefore, the algorithms are suitable for applications such as online control of FES based neuroprostheses by a brain-computer interface. Tests are performed with datasets recorded from two subjects for artifact durations ranging from 0.5 ms to 10 ms. After application of the artifact removal algorithms the signal-to-noise ratio of the reconstructed signals ranges from 15 dB to 45 dB, depending on the duration of artifacts and the type of algorithm.**

I. INTRODUCTION

Surface functional electrical stimulation (FES) is a technique which uses electrodes attached to the skin to activate nerves. Short, pulsed currents are applied to the electrodes and trigger action potentials in the nerves under the electrodes. Many applications of FES exist, including restitution of upper- or lower-limb function after spinal cord injury, and rehabilitation of upper- or lower-limb function after stroke. Since FES activates nerves, the effects of FES can be observed in the stimulated nerves, in muscles or organs innervated by the stimulated nerves, and in the central nervous system (through activation of afferent nerves and through proprioception).

While basic effects of FES nowadays are well understood, many questions regarding the effect of FES on brain activity remain unanswered. Therefore, studying the immediate and long-term effects of FES on brain activity is an interesting and timely research topic. A simple but effective neuroimaging method, which can be used for such studies is the electroencephalogram (EEG). However, the study of immediate effects of FES on brain activity is hampered by so-called stimulation artifacts appearing in the EEG when it is recorded while stimulation takes place. The stimulation artifacts can be several orders of magnitude larger than the physiologic EEG activity, and therefore techniques for the removal of stimulation artifacts from EEG are needed.

U. Hoffmann and T. Keller are with the Department of Rehabilitation, Health Technologies Unit, Tecnalia, 20009 San Sebastián, Spain

Email of corresponding author: ulrich.hoffmann@tecnalia.com

A. Ramos is with Tecnalia Germany and the Institute of Medical Psychology and Behavioral Neurobiology, University of Tübingen, 72074 Tübingen, Germany

W. Cho is with the Institute of Medical Psychology and Behavioral Neurobiology, University of Tübingen, 72074 Tübingen, Germany

Previous studies concerning the removal of stimulation artifacts from electrophysiological signals have focused on modifications of the measurement setup and hardware used for recording signals, as well as on algorithm development for removing artifacts. Concerning modifications of the measurement setup, three recommendations can be found in the literature: a) maximization of the distance between stimulation and recording electrode, b) use of ground straps connecting subject and amplifier to the ground, and c) proper skin preparation and use of non-polarizable electrodes [1], [2]. These techniques reduce artifact amplitude by respectively reducing volume conducted currents (a), displacement currents (b), and electromagnetically coupled currents (c) generated during stimulation [1], [2].

Several studies contain reports about specifically constructed amplifiers and stimulators (e.g [3], [4]). A simple example are recording amplifiers which can be synchronized with the stimulator and which switch to sample and hold mode during artifacts [3]. Another hardware based technique employs stimulators which use a constant voltage output stage between stimulation pulses and a constant current output stage during stimulation [4]. This allows to reduce the duration of artifacts but does not necessarily reduce the amplitude of artifacts.

An alternative to hardware based methods are algorithms for artifact removal. The main advantages of such algorithms are that recordings can be done with standard hardware and that algorithms can be flexibly adapted to different artifact parameters and recording situations. Many algorithms compute estimates of the shape of stimulation artifacts and subtract the estimated artifact shape from the recordings. An example is the algorithm described in [5], in which the artifact shape is determined by averaging over individual artifacts. Another example is the algorithm described in [6], in which the artifact shape is computed by averaging artifacts with exponential forgetting. The main disadvantage of such algorithms is that it is inherently difficult to obtain an estimate of the quality of the signals after artifact removal. This is so because the ground-truth signal, i.e. the signal without artifacts cannot be measured. Furthermore, the amplitude and shape of artifacts resulting from FES can fluctuate rapidly and strongly, making the precise fitting of artifacts a difficult task.

Subtraction based algorithms concentrate on modeling the artifacts. However, it is also possible to focus on modeling artifact-free electrophysiological signals. Algorithms following this approach replace the measurements affected by artifacts with values interpolated from non-contaminated

978-1-4244-4122-8/11/$26.00 ©2011 IEEE

portions of the signal. This has the advantage that reliable estimates of the quality of the signal after artifact removal can be obtained. To obtain such estimates it is sufficient to remove small portions from a clean signal, to interpolate the removed portions, and to compare the interpolation with the true signal. A further advantage is that artifact removal based on modeling artifact-free signals does not depend on the shape of artifacts. Hence, the same algorithm can be applied for signals recorded during stimulation with different parameters (e.g. stimulation with varying pulse width). An example for the signal modeling approach to artifact removal, is a frequency domain implementation applied to EEG signals recorded during deep brain stimulation in Parkinsons patients [7].

Here, we present and compare two simple time-domain methods for removing stimulation artifacts from the EEG. Both methods consist of a module for artifact detection and of a module for interpolating missing samples from neighboring samples. The algorithms have been designed to require only relatively little computational power and are in principle suitable for online application during the recording of signals. This is important in applications such as FES for grasping controlled by a brain-computer interface [8] and other bio-feedback applications combining EEG and FES.

The outline of the rest of this article is as follows. In Section II details about the hardware and experiment setup used for recording EEG and performing FES stimulation are described. Furthermore, examples of the typical shape of stimulation artifact in EEG records are given. In Section III algorithms for detecting and removing artifacts from EEG signals are described. Results are given in Section IV, and are discussed in Section V.

II. Experiment Setup

To test the algorithms described in this paper, EEG datasets were recorded from two subjects without known neurological deficits (S1 female, age 23 years; S2 male, age 36 years). From both subjects data was recorded in two conditions.

In condition I, a Compex Motion stimulator [9] was used to apply FES to the forearm of the subjects, with the active electrode positioned close to the motor point of the extensor muscles of the wrist. Stimulation trains with a duration of approximately 3 seconds were applied between seconds 3 and 6 of 10 second long trials. Stimulation frequency was set to 35 Hz, biphasic pulses were employed, and the pulse width was linearly increased from 0 μs to 300 μs during the first second of stimulation, then held constant for one second, and decreased from 300 μs to 0 μs during the last second. The stimulation current was set individually for each subject to evoke well-defined wrist movements. For each subject 40 trials were recorded in condition I.

In condition II, a paradigm typically used in motor imagery experiments was employed. Trials had a duration of 10 s and in each trial subjects were instructed to imagine either left-hand movement, right-hand movement, or to relax. For subject S1, 120 trials (40 left-hand, 40 right-hand, 40 relax) were recorded and for subject S2, 90 trials (30 left-hand, 30 right-hand, 30 relax) were recorded.

To record EEG signals a g.Tec g.USBamp amplifier was used. Sampling frequency was set to 2.4 kHz, the reference electrode was attached to the right mastoid and the ground electrode to the left mastoid. Sixteen recording electrodes were distributed over the motor cortex and the parietal cortex. Electrode impedance was kept below 5 kOhm for all electrodes. Examples of the recorded artifacts are shown in Fig. 1.

III. Algorithms

A. Detection of Artifacts

Stimulation artifacts in EEG recordings consist of sharp, high-amplitude spikes, occurring simultaneously on all recording channels. The artifact detection algorithm presented here exploits these characteristics by computing first order differences in each recording channel and by summing up the first order differences over channels. Denoting by $x_c(t)$ the EEG signal recorded from channel c at time t and by C the number of channels, this can be expressed as follows:

$$d(t) = \sum_{c=1}^{C} x_c(t+1) - x_c(t) \qquad (1)$$

In the resulting one-channel signal $d(t)$ the artifacts are well represented and can be reliably detected. An algorithm which has been proposed for the detection of spikes from recordings of neuronal spiking activity (multiunit recordings) is used for this [10]. The first step in this algorithm is to compute the median absolute deviation of the input signal in a sliding window. Denoting by $\mathcal{W}(t) = \{t-W, t-W+1, \dots t+W\}$ a window of length $2W+1$ samples, centered at t, this can be expressed as:

$$m(t) = \operatorname*{med}_{i \in \mathcal{W}(t)} |d(i) - \operatorname*{med}_{j \in \mathcal{W}(t)} d(j)| \qquad (2)$$

Samples of $d(t)$ are flagged as belonging to artifacts whenever the absolute value of $d(t)$ is above a threshold set to a multiple of the median absolute deviation:

$$a(t) = \begin{cases} 1 & \text{if } |d(t)| > \alpha m(t) \\ 0 & \text{if } |d(t)| \leq \alpha m(t) \end{cases} \qquad (3)$$

As a last step, the detections in $a(t)$ are clustered and extended using three rules:

- If none of the D samples before a detection at t is flagged as artifact, $a(t-1)$ and $a(t-2)$ are set to 1.
- If none of the D samples after a detection at t is flagged as artifact, $a(t+1)$ and $a(t+2)$ are set to 1.
- If two detections are less than D samples apart, the samples between the detections are flagged as artifacts.

B. Removal of Artifacts Using Linear Interpolation

Linear interpolation is a simple and straight-forward method to interpolate samples flagged as artifacts. Denoting by $x_c(t_s)$ the value of the last sample before the artifact and by $x_c(t_e)$ the value of the first sample after the artifact, linear

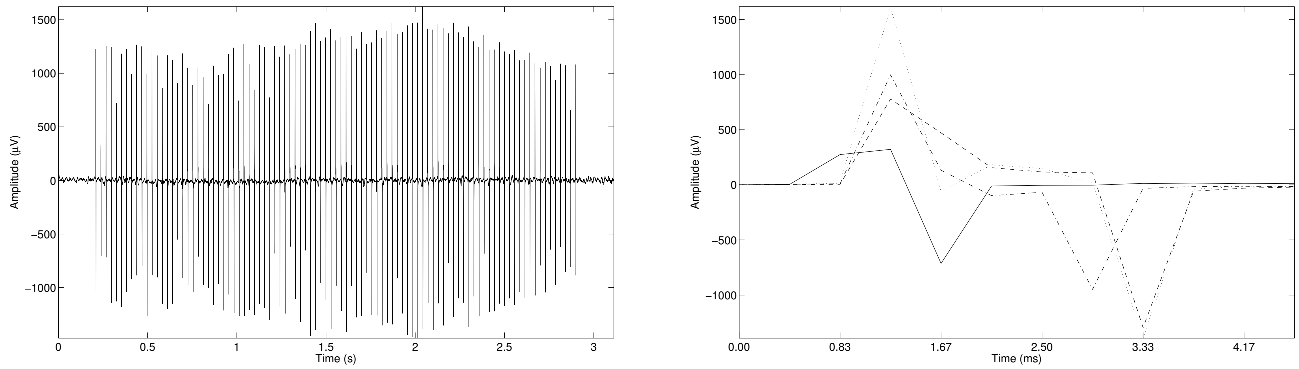

Fig. 1. Examples of stimulation artifacts. Left: Pulse train resulting from stimulation with the parameters described in Section II. Right: Detailed view of 4 single artifacts from the pulse train. The artifacts have amplitudes of up to 1.5 mV, duration of about 4 ms, and show significant variations in shape and amplitude.

interpolation of samples with $t \in \{t_s+1, t_s+2, \ldots, t_e-1\}$ is accomplished as follows:

$$\tilde{x}_c(t) = \frac{x_c(t_e)(t-t_s)}{t_e-t_s} + \frac{x_c(t_s)(t_e-t)}{t_e-t_s} \tag{4}$$

C. Removal of Artifacts Using a Gaussian Distribution

A more powerful approach than linear interpolation is described in the following. The algorithm works by learning a Gaussian probability density of short multi-channel segments of EEG from artifact-free training data. This probability density is used to infer the conditional density of samples affected by artifacts from neighboring non-contaminated samples.

To learn the Gaussian density, short segments of multichannel EEG containing data from T temporal samples and C channels were extracted from the training data[1]. Each multichannel segment was normalized by subtracting the mean in each channel, and by setting the variance of each channel to 1. As a final preprocessing step, column vectors of dimension $TC \times 1$ were formed from the normalized multichannel segments. Denoting the training vectors resulting from this procedure by $\mathbf{z}_i$ and the number of training vectors by N, the sample mean $\mathbf{m}$ and covariance matrix $\mathbf{\Sigma}$ are computed as follows:

$$\mathbf{m} = \frac{1}{N}\sum_{i=1}^{N}\mathbf{z}_i, \quad \mathbf{\Sigma} = \frac{1}{N}\sum_{i=1}^{N}(\mathbf{z}_i-\mathbf{m})^T(\mathbf{z}_i-\mathbf{m}) \tag{5}$$

The probability density of a EEG segment $\mathbf{z}$ can then be expressed as:

$$p(\mathbf{z}|\mathbf{m},\mathbf{\Sigma}) = \frac{1}{(2\pi)^{TC/2}|\mathbf{\Sigma}|^{1/2}} e^{-\frac{1}{2}(\mathbf{z}-\mathbf{m})^T\mathbf{\Sigma}^{-1}(\mathbf{z}-\mathbf{m})} \tag{6}$$

If only R samples in $\mathbf{z}$ can be reliably measured, the probability density for the missing part is again Gaussian and can be easily computed from the full density of the training data. We denote by $\mathbf{x}$ the part of $\mathbf{z}$ which can be reliably measured, and by $\mathbf{y}$ the the samples affected by an artifact:

$$\mathbf{z} = \begin{bmatrix} \mathbf{x} \\ \mathbf{y} \end{bmatrix} \tag{7}$$

The probability density at $\mathbf{y}$ given $\mathbf{x}$ is then:

$$p(\mathbf{y}|\mathbf{x},\hat{\mathbf{m}},\hat{\mathbf{\Sigma}}) = \frac{1}{(2\pi)^{\frac{TC-R}{2}}|\hat{\mathbf{\Sigma}}|^{\frac{1}{2}}} e^{-\frac{1}{2}(\mathbf{y}-\hat{\mathbf{m}})^T\hat{\mathbf{\Sigma}}^{-1}(\mathbf{y}-\hat{\mathbf{m}})} \tag{8}$$

To compute $\hat{\mathbf{m}}$ and $\hat{\mathbf{\Sigma}}$, $\mathbf{m}$ and $\mathbf{\Sigma}$ are split into portions corresponding to the observed and unobserved parts of $\mathbf{z}$:

$$\mathbf{m} = \begin{bmatrix} \mathbf{a} \\ \mathbf{b} \end{bmatrix}, \quad \mathbf{\Sigma} = \begin{bmatrix} \mathbf{A} & \mathbf{C} \\ \mathbf{C}^T & \mathbf{B} \end{bmatrix} \tag{9}$$

The mean and covariance of the conditional density can then be computed as follows:

$$\hat{\mathbf{m}} = \mathbf{b} + \mathbf{C}^T\mathbf{A}^{-1}(\mathbf{x}-\mathbf{a}), \quad \hat{\mathbf{\Sigma}} = \mathbf{B} - \mathbf{C}^T\mathbf{A}^{-1}\mathbf{C} \tag{10}$$

The samples affected by an FES artifact can now simply be replaced by the corresponding values from $\hat{\mathbf{m}}$.

IV. Results

A. Detection of Artifacts

To evaluate the performance of the artifact detection algorithm, the data recorded in condition I, i.e. the data recorded with FES stimulation was used (cf. Section II). The detection performance was evaluated in terms of true positives (correctly detected artifacts), false positives (detections without artifacts), and false negatives (undetected artifacts). The number of true positives was defined as the number of detected artifacts having the following characteristics:

- Duration more than 3 ms and less than 7 ms
- Distance to neighboring detections in the range $\frac{1}{F_s} - 2$ ms to $\frac{1}{F_s} + 2$ ms (F_s = 35 Hz)

False positives were defined as all detections not fulfilling the above characteristics. The number of false negatives was defined by computing from the stimulation parameters the expected number of artifacts for each trial and by subtracting the number of true positives.

The results of the evaluation showed that on the test data all artifacts were detected and no false detections occurred.

[1] T was set to 110 samples in the experiments reported here.

B. Removal of Artifacts

The datasets recorded in condition II (cf. Section II) were used to evaluate the performance of the artifact removal algorithms. To this end, in each trial artificial artifacts were inserted in each channel at time points $t = 3 + \frac{i}{F_s}$ s, where $i \in 0 \ldots 94$ and $F_s = 35$ Hz, i.e. the temporal distribution of the artificial artifacts was equivalent to the temporal distribution of the true artifacts observed in the datasets recorded in condition I. The duration of artificial artifacts was varied between 1 sample (0.412 ms) and 24 samples (10 ms). Since the algorithm for detection of artifacts was independently evaluated with the datasets recorded in experiment condition I , artificial artifacts were simply represented by NaNs.

After inserting artificial artifacts, the algorithms described in Section III were applied to interpolate the EEG in the intervals where the artificial artifacts were inserted. The resulting data was then lowpass filtered with a cut-off frequency of 45 Hz, and offset and trend were removed from each trial. The same procedure, i.e. lowpass filtering and removal of offset and trend was applied to the original data recorded in condition II. The lowpass filtering and removal of offset and trend was done in order to mimic typical steps applied in EEG analysis and to ensure a realistic performance evaluation of the algorithms.

The noise signal obtained by subtracting the filtered and detrended original data from the filtered and detrended data after artifact removal was used to quantify the performance of the algorithms. Denoting by $x_c(t)$ the original data (after detrending and filtering) and by $\tilde{x}_c(t)$ the data after artifact removal, the difference signal $n_c(t)$ is:

$$n_c(t) = x_c(t) - \tilde{x}_c(t). \tag{11}$$

Using the noise signal and the true signal the signal-to-noise ratio (in decibel) was computed for each trial:

$$s = 10 \log_{10} \frac{\sum_{c=1}^{C} \sum_{t=t_1}^{t_2} x_c(t)^2}{\sum_{c=1}^{C} \sum_{t=t_1}^{t_2} n_c(t)^2}. \tag{12}$$

The parameters t_1 and t_2 were set to include only the parts of each trial affected by artifacts (seconds 3 to 6, cf. Section II.). As an additional performance parameter the maximal amplitude of the noise was determined for each trial:

$$p = \max_{t \in \{t_1, t_1+1 \ldots t_2\}, c \in \{1,2,\ldots C\}} |n_c(t)| \tag{13}$$

Since the artifact removal algorithm based on Gaussian density modeling relies on training data, 10 trials from each of the datasets recorded in condition II were set aside for training. The rest of the trials was used for performance evaluation. The signal-to-noise ratio averaged over all trials and the average peak noise are shown in Fig. 2.

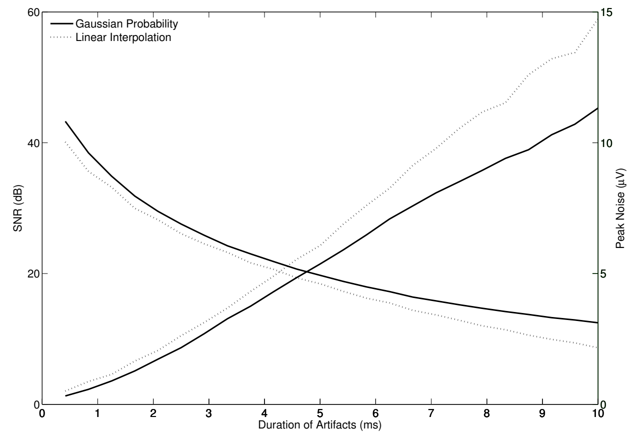

Fig. 2. Average signal-to-noise ratio and average peak noise amplitude obtained with the algorithms described in Section III.

V. CONCLUSION

The results show that comparatively simple artifact removal algorithms allow to obtain good quality signals from artifact-contaminated EEG recordings. The test data contained only artifacts with high amplitudes and hence further tests are necessary to see how artifact detection works with lower amplitude artifacts. Further improvements in the signal-to-noise ratio might be achieved by tracking the probability density of EEG signals over time, e.g. with a Kalman filter. However, the applicability of such methods for online artifact removal has to be critically examined because the requirements in terms of computation time increase.

VI. ACKNOWLEDGMENTS

This work has been partially supported by projects DPI2009-14732-C02-02 and HYPER-CSD2009-00067 funded by the Spanish Government.

REFERENCES

[1] L. McLean, R. N. Scott, and P. A. Parker, Stimulus Artifact Reduction in Evoked Potential Measurements, *Arch. Phys. Med. Rehabil.*, vol. 77, 1996, pp 1286 - 1292.

[2] K. C. McGill, K. L. Cummins, L. J. Dorfman, B. B. Berlizot, K. Luetkemeyer, D. G. Nishimura, and B. Widrow, On the Nature and Elimination of Stimulus Artifact in Nerve Signals Evoked and Recorded Using Surface Electrodes, *IEEE Trans. Biomed. Eng.*, vol. 29, 1982, pp 129 - 136.

[3] J. A. Freeman, An electronic stimulus artifact suppressor, *Electroenceph. Clin. Neurophys.* vol. 31 , 1971, pp 170 - 172.

[4] F. D. Pozo, J. M. R. Delgado, Hybrid stimulator for chronic experiments, *IEEE Trans. Biomed. Eng.*, vol. 25, 1978, pp 92 - 95.

[5] T. Wichmann, A digital averaging method for removal of stimulus artifacts in neurophysiologic experiments, *J Neur. Meth.*, vol. 98, 2000, pp 57 - 62.

[6] T. Keller, M. R. Popovic, Real-time stimulation artifact removal in EMG signals for neuroprosthesis control applications, *in IFESS 2001, 6th Annual Conference of the International Functional Electrical Stimulation Society*, Cleveland, 2001.

[7] D. P. Allen, E. L. Stegemöller, C. Zadikoff, J. M. Rosenow, and C. D. MacKinnon, Suppression of deep brain stimulation artifacts from the electroencephalogram by frequency domain Hampel filtering, *Clin. Neurophys.*, vol. 121, 2010, 1227 - 1232.

[8] G. Pfurtscheller, G. R. Müller, J. Pfurtscheller, H. J. Gerner, and R. Rupp, Thought-control of functional electrical stimulation to restore hand grasp in a patient with tetraplegia, *Neuroscience Letters*, vol. 351, pp 33 - 36

[9] T. Keller, M. R. Popovic, I. P. Pappas, and P. Y. Müller, Transcutaneous functional electrical stimulator "Compex Motion", *Artif. Organs*, vol. 26, 2002, pp 219 - 223.

[10] R. Quian Quiroga, Z. Nadasy, and Y. Ben-Shaul, Unsupervised Spike Detection and Sorting with Wavelets and Superparamagnetic Clustering, *Neural Computation*, vol. 16, 2004, pp 1661 - 1687.